Simulation of the Stationary Nonisothermal MHD Flows of Polymeric Fluids in Channels with Interior Heating Elements

A. M. Blokhin[1,2*] and B. V. Semisalov[3,2**]

[1]*Sobolev Institute of Mathematics, pr. Akad. Koptyuga 4, Novosibirsk, 630090 Russia*

[2]*Novosibirsk State University, ul. Pirogova 1, Novosibirsk, 630090 Russia*

[3]*Federal Research Center for Information and Computational Technologies,
pr. Akad. Lavrent'eva 6, Novosibirsk, 630090 Russia*

Abstract—Basing on the rheological mesoscopic Pokrovskii–Vinogradov model, the equations of nonrelativistic magneto-hydrodynamics, and the heat conduction equation with dissipative terms, we obtain a closed coupled system of nonlinear partial differential equations that describes the flow of solutions and melts of linear polymers. We take into account the rheology and induced anisotropy of a polymeric fluid flow as well as mechanical, thermal, and electromagnetic impacts. The parameters of the equations are determined by mechanical tests with up-to-date materials and devices used in additive technologies (as $3D$ printing). The statement is given of the problems concerning stationary polymeric fluid flows in channels with circular and elliptical cross-sections with thin inclusions (some heating elements). We show that, for certain values of parameters, the equations can have three stationary solutions of high order of smoothness. Just these smooth solutions provide the defect-free additive manufacturing. To search for them, some algorithm is used that bases on the approximations without saturation, the collocation method, and the relaxation method. Under study are the dependences of the distributions of the saturation fluid velocity and temperature on the pressure gradient in the channel.

INTRODUCTION

As is known [1], the solutions and melts of linear polymers are nonlinear viscoelastic media. In the article, we consider some model of the dynamics of these media that is a modification of the well-known rheological mesoscopic model due to Pokrovskii–Vinogradov [1-3] describing complex rheology and induced anisotropy of polymer solutions and melts with high degree of accuracy. In Section 1, the equations of the model with dimensionless variables are presented that also account for the influence of temperature and electromagnetic fields, which is impotant for solving the problems of many applied fields; in particular, the problems related to the development and improvement of technology of additive manufacturing ($3D$ printing) of polymer-based products.

The first natural step in studying the described model is to identify the characteristic regimes of the stationary flow of polymers which are close in the qualitative features to the well-known Poiseuille flows for the system of Navier–Stokes equations (see [4] and Section 2). In particular, these flow regimes occur in the channels of printing devices at continuous supply of ink. Note that, for certain parameter values, the model admits the multiplicity of stationary smooth solutions (see Section 3). As a rule, the channels have circular or elliptical cross-section and include some internal heating elements. The statement of the boundary value problems in the domains of this type is described in Section 4.

[*]E-mail: blokhin@math.nsc.ru

[**]E-mail: vibis@ngs.ru

Identification of the parameters of the developed model and formulated problems rests upon the data of the mechanical tests that involve up-to-date materials and devices used in additive technologies. These data are obtained from a wide set of sources [5−15]; their consolidated table as well as a brief summary are presented in the Appendix.

For numerical solution of the nonlinear boundary value problems with given parameters, the nonlocal method without saturation is used [16, 17] with application of the Chebyshev and Fourier approximations. This method allows us to carry out calculations with rather low consumption of memory and computer time and the error control in the problems with highly smooth solutions [18, 19]. The graphs of numerical solutions and comments to them are given in Section 5 together with some discussion of flow properties in dependence on the pressure gradient in the channel.

1. A MODIFIED POKROVSKII−VINOGRADOV MODEL

Following the monographs [1, 2, 4, 20−22] and articles [23, 24], we derive the equations of the *modified rheological Pokrovskii−Vinogradov model* which describes nonisothermal magneto-hydrodynamic (hereinafter MHD) flow of an incompressible viscoelastic polymeric fluid and takes into account the heat dissipation. In dimensionless form in a rectangular Cartesian coordinate system (x, y, z) these equations are as follows:

$$\text{div } \mathbf{u} = 0, \tag{1}$$

$$\text{div } \mathbf{H} = 0, \tag{2}$$

$$\frac{d\mathbf{u}}{dt} + \nabla\left(P + \frac{\sigma_m \|\mathbf{H}^2\|}{2}\right) = \frac{1}{\text{Re}} \text{div}(Y\Pi) + \sigma_m(\mathbf{H}, \nabla)\mathbf{H} + \text{Ga}(Y - 1)\begin{pmatrix} 1 \\ 0 \\ 0 \end{pmatrix}, \tag{3}$$

$$\frac{d\mathbf{H}}{dt} = (\mathbf{H}, \nabla)\mathbf{u} + b_m \mathbf{\Delta_{x,y,z}H}, \tag{4}$$

$$\frac{da_{11}}{dt} - 2A_1 u_x - 2a_{12}u_y - 2a_{13}u_z + \mathfrak{L}_{11} = 0, \tag{5}$$

$$\frac{da_{22}}{dt} - 2a_{12}v_x - 2A_2 v_y - 2a_{23}v_z + \mathfrak{L}_{22} = 0, \tag{6}$$

$$\frac{da_{33}}{dt} - 2a_{13}w_x - 2a_{23}w_y - 2A_3 w_z + \mathfrak{L}_{33} = 0, \tag{7}$$

$$\frac{da_{12}}{dt} + w_z a_{12} - A_1 v_x - A_2 u_y - v_z a_{13} - u_z a_{23} + \mathfrak{L}_{12} = 0, \tag{8}$$

$$\frac{da_{13}}{dt} - w_y a_{12} - A_1 w_x - A_3 u_z + v_y a_{13} - u_y a_{23} + \mathfrak{L}_{13} = 0, \tag{9}$$

$$\frac{da_{23}}{dt} + u_x a_{23} - A_2 w_y - A_3 v_z - w_x a_{12} - v_x a_{13} + \mathfrak{L}_{23} = 0, \tag{10}$$

$$\frac{dY}{dt} = \frac{1}{\text{Pr}}(\Delta_{x,y,z}Y + AY\Phi + A_m\Phi_m). \tag{11}$$

Here t is time; u, v, and w are the components of the velocity vector $\mathbf{u}$ in the Cartesian coordinate system x, y, and z; $\mathbf{H} = (L, M, N)$ is the vector of the magnetic field intensity; P is the pressure; a_{ij}, $i, j = 1, 2, 3$, are the components of the second rank symmetric anisotropy tensor Π; $\mathbf{a_1}$, $\mathbf{a_2}$, and $\mathbf{a_3}$ are the columns of the symmetric matrix $\Pi = (a_{ij}) = (\mathbf{a_1}, \mathbf{a_2}, \mathbf{a_3})$; $\|\mathbf{a_i}\|^2 = (\mathbf{a_i}, \mathbf{a_i})$, $i = 1, 2, 3$;

$$\text{div}(Y\Pi) = (\text{div}(Y\mathbf{a_1}), \text{div}(Y\mathbf{a_2}), \text{div}(Y\mathbf{a_3}))^\top;$$

and $Y = T/T_0$, T is the temperature, $T_0 = 293.15$ K $= 20°$ C is the environment temperature;

$$\mathfrak{L}_{ij} = (K_I a_{ij} + \beta(\mathbf{a_i}, \mathbf{a_j}))/\bar{\tau}_0(Y), \qquad i, j = 1, 2, 3;$$

$K_I = W^{-1} + \bar{k}/3\, I$, $\bar{k} = k - \beta$, $I = (a_{11} + a_{22} + a_{33})$ is the first invariant of the anisotropy tensor Π, $A_i = a_{ii} + W^{-1}$, $i = 1, 2, 3$; k and β, $0 < \beta < 1$, are the phenomenological parameters of the model

that characterize the contributions related to anisotropy (β takes into account the orientation of the macromolecular coil, while k stands for its size [1]);

$$\bar{\tau}_0 = \frac{J(Y)}{Y}, \qquad J(Y) = \exp\left(-\overline{E}_A\frac{Y-1}{Y}\right);$$

$\mathrm{Re} = \rho u_H l/\eta_0^*$ is the Reynolds number, $\rho = \mathrm{const}$ is the density of the medium; $\mathrm{W} = \tau_0^* u_H/l$ is the Weissenberg number; η_0^* and τ_0^* are the initial values of the shear viscosity and the relaxation time at $T = T_0$ [1, 5]; Φ and Φ_m are the dissipative functions (see Remark 2); the Laplace operator $\Delta_{x,y,z}$ has the form

$$\Delta_{x,y,z} = \left(\frac{\partial^2}{\partial x^2} + \frac{\partial^2}{\partial y^2} + \frac{\partial^2}{\partial z^2}\right) = \left(\frac{\partial^2}{\partial x^2} + \Delta_{y,z}\right);$$

$$\Delta_{\mathbf{x,y,z}}\mathbf{H} = (\Delta_{x,y,z}L, \Delta_{x,y,z}M, \Delta_{x,y,z}N)^\top; \qquad \frac{d}{dt} = \frac{\partial}{\partial t} + (\mathbf{u}, \nabla),$$

where for arbitrary vector-functions $\mathbf{q} = (q_1, q_2, q_3)$ and $\mathbf{s} = (s_1, s_2, s_3)$ the vector $(\mathbf{q}, \nabla)\mathbf{s}$ has the form

$$(\mathbf{q}, \nabla)\mathbf{s} = \left(q_1\frac{\partial s_1}{\partial x} + q_2\frac{\partial s_1}{\partial y} + q_3\frac{\partial s_1}{\partial z}, \quad q_1\frac{\partial s_2}{\partial x} + q_2\frac{\partial s_2}{\partial y} + q_3\frac{\partial s_2}{\partial z}, \quad q_1\frac{\partial s_3}{\partial x} + q_2\frac{\partial s_3}{\partial y} + q_3\frac{\partial s_3}{\partial z}\right)^\top;$$

$\mathrm{Ga} = \mathrm{Ra}\,/\,\mathrm{Pr}$, $\overline{E}_A = E_A/T_0$; the Rayleigh number Ra, the Prandtl number Pr, and the activation energy E_A are described in [4]; A and A_m are the dissipation coefficients of the heat equation (11); $\sigma_m = \mu_0 H_0^2/(\rho u_H^2)$ is the magnetic pressure coefficient; $b_m = 1/\mathrm{Re}_m$, $\mathrm{Re}_m = \sigma_e\mu_0 u_H l$ is the magnetic Reynolds number; μ_0 is the magnetic permeability of vacuum; and σ_e is the electrical conductivity of the medium.

System (1)–(11) is written in dimensionless form, where the time t, the coordinates x, y, and z, the velocity vector components u, v, and w, the pressure P, the components of the vector of the magnetic field intensity L, M, and N, and the components of the anisotropy tensor a_{ij} are normalized by l/u_H, l, u_H, ρu_H^2, H_0, and $W/3$, respectively, where l is the characteristic length, u_H is the characteristic velocity, and H_0 is the characteristic value of the magnetic field intensity.

It was possible to identify the most parameters of the above model using the results of mechanical tests with certain polymer materials and $3D$ printing devices. These values with the links to sources and comments are given in the Appendix.

Remark 1. Magnetohydrodynamic equations (1)–(11) are derived involving the system of Maxwell's equations [20, 21], whereas the magnetic induction vector $\mathbf{B}$ is taken in the form $\mathbf{B} = \mu_0\mathbf{H}$. In fact, the more general formula holds [25, 26]:

$$\mathbf{B} = \mu\mu_0\mathbf{H} = (1 + \chi)\mu_0\mathbf{H}, \tag{12}$$

where μ is the magnetic permeability χ is the magnetic susceptibility, and moreover

$$\chi = \chi_0/Y, \tag{13}$$

χ_0 is the magnetic susceptibility at $T = T_0$.

Remark 2. Following [27], we use the binary tensor operation ":" to specify the dissipative functions Φ and Φ_m in (11):

$$\Phi = \Pi : \nabla\mathbf{u} := \sum_{i,j=1}^{3} a_{ij}\frac{\partial u_j}{\partial x_i} = a_{11}\frac{\partial u_1}{\partial x_1} + \left(\frac{\partial u_1}{\partial x_2} + \frac{\partial u_2}{\partial x_1}\right)a_{12}$$

$$+ \left(\frac{\partial u_1}{\partial x_3} + \frac{\partial u_3}{\partial x_1}\right)a_{13} + a_{22}\frac{\partial u_2}{\partial x_2} + \left(\frac{\partial u_2}{\partial x_3} + \frac{\partial u_3}{\partial x_2}\right)a_{23} + a_{33}\frac{\partial u_3}{\partial x_3}, \tag{14}$$
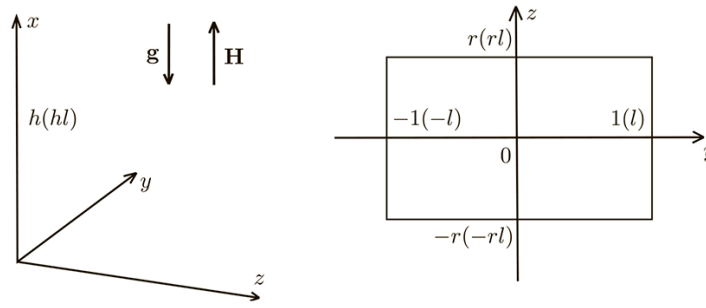
Fig. 1. A channel with rectangular section.

$$\Phi_m = \sigma_m \Pi_m : \nabla \mathbf{u} := \sigma_m \sum_{i,j=1}^{3} L_i L_j \frac{\partial u_j}{\partial x_i} = \sigma_m \left\{ L_1^2 \frac{\partial u_1}{\partial x_1} + \left(\frac{\partial u_1}{\partial x_2} + \frac{\partial u_2}{\partial x_1} \right) L_1 L_2 \right.$$

$$\left. + \left(\frac{\partial u_1}{\partial x_3} + \frac{\partial u_3}{\partial x_1} \right) L_1 L_3 + L_2^2 \frac{\partial u_2}{\partial x_2} + \left(\frac{\partial u_2}{\partial x_3} + \frac{\partial u_3}{\partial x_2} \right) L_2 L_3 + L_3^2 \frac{\partial u_3}{\partial x_3} \right\}. \tag{15}$$

Here $u_1(=u)$, $u_2(=v)$, $u_3(=w)$ and $L_1(=L)$, $L_2(=M)$, $L_3(=N)$ are the components of the velocity vector $\mathbf{u}$ and the intensity vector $\mathbf{H}$ in the Cartesian coordinate system $x_1(=x)$, $x_2(=y)$, $x_3(=z)$; and $\Pi_m = (L_i L_j)$ for $i, j = 1, 2, 3$.

Remark 3. According to [28, 29], (1)–(11) should be supplemented by boundary conditions for the velocity vector components (no-slip condition on the channel wall) as well as for the temperature and magnetic field components on the channel walls. Below we obtain the resolving equations for the above variables in the channels with circular and elliptical cross-sections and internal heating elements. We give a specific type of boundary conditions for each problem.

As in [28, 29], we look for a particular solution to the original system (1)–(11) of the following form:

$$v = w \equiv 0, \qquad u = \hat{u}(y, z),$$
$$P = \widehat{P}(x, y, z) = \mathcal{S}(y, z) - \hat{A}x, \tag{16}$$
$$a_{ij} = \hat{a}_{ij}(y, z), \quad i, j = 1, 2, 3, \qquad Y = \widehat{Y}(y, z).$$

Moreover, assume that $M = N = 0$ and $L = \hat{L}(y, z)$. Such a situation is realized when a channel is wound with an electric wire or immersed into a coil.

Solution (16) corresponds to a stationary flow of a polymeric fluid in a channel with rectangular cross section under the action of the constant pressure drop $\widehat{\Delta P}$ along the channel axis (see Fig. 1). Here

$$\widehat{P}_x = -\hat{A}(= \text{const}) = \frac{1}{\text{Re}} \{ (\widehat{Y}\hat{a}_{12})_y + (\widehat{Y}\hat{a}_{13})_z \} + \text{Ga}(Y - 1) + \hat{L}\hat{L}_x, \quad \hat{A} = \frac{\widehat{\Delta P}}{\rho u_H^2 h}, \quad \hat{L}_x = 0,$$

where $-\widehat{\Delta P}/(\rho u_H^2)$ is the dimensionless pressure drop on the segment h, while the dimensional quantity is positive, $\widehat{\Delta P} > 0$. To determine the functions $\hat{u}$, $\mathcal{S}$, $\hat{a}_{ij}$, and $\widehat{Y}$ (see (16)) from (3)–(11), we arrive at the following relations:

$$(\widehat{Y}\hat{a}_{12})_y + (\widehat{Y}\hat{a}_{13})_z = -\widehat{D} = -\text{Re}[\hat{A} + \text{Ga}(\widehat{Y} - 1)], \tag{17}$$

$$\mathcal{S}_y = \frac{1}{\text{Re}}[(\widehat{Y}\hat{a}_{22})_y + (\widehat{Y}\hat{a}_{23})_z] - \sigma_m \hat{L}\hat{L}_y, \qquad \mathcal{S}_z = \frac{1}{\text{Re}}[(\widehat{Y}\hat{a}_{23})_y + (\widehat{Y}\hat{a}_{33})_z] - \sigma_m \hat{L}\hat{L}_z, \tag{18}$$

$$\Delta_{y,z}\hat{L} = 0, \tag{19}$$

$$K_{\hat{I}}\hat{a}_{11} + \beta\|\hat{\mathbf{a}_1}\|^2 = 2\bar{\tau}_0(\widehat{Y})(\hat{a}_{12}\hat{u}_y + \hat{a}_{13}\hat{u}_z), \tag{20}$$

$$K_{\hat{I}}\hat{a}_{22} + \beta\|\hat{\mathbf{a}_2}\|^2 = 0, \qquad K_{\hat{I}}\hat{a}_{33} + \beta\|\hat{\mathbf{a}_3}\|^2 = 0, \tag{21}$$

$$K_{\hat{I}}\hat{a}_{12} + \beta(\hat{\mathbf{a}_1}, \hat{\mathbf{a}_2}) = \bar{\tau}_0(\widehat{Y})(\hat{A}_2\hat{u}_y + \hat{a}_{23}\hat{u}_z), \tag{22}$$

$$K_{\hat{I}}\hat{a}_{13} + \beta(\hat{\mathbf{a}_1}, \hat{\mathbf{a}_3}) = \bar{\tau}_0(\widehat{Y})(\hat{A}_3\hat{u}_z + \hat{a}_{23}\hat{u}_y), \tag{23}$$

$$K_{\hat{I}}\hat{a}_{23} + \beta(\hat{\mathbf{a}_2}, \hat{\mathbf{a}_3}) = 0, \tag{24}$$

$$\Delta_{y,z}\widehat{Y} + A\widehat{Y}\widehat{\Phi} = 0. \tag{25}$$

Here $K_{\hat{I}} = W^{-1} + \bar{k}/3\hat{I}$, $\hat{I} = \hat{a}_{11} + \hat{a}_{22} + \hat{a}_{33}$, $\hat{A}_i = W^{-1} + \hat{a}_{ii}$ for $i = 2, 3$; and $\widehat{\Phi} = \hat{u}_y\hat{a}_{12} + \hat{u}_z\hat{a}_{13}$.

Note that, by (15), in this formulation $\widehat{\Phi}_m = 0$.

Remark 4. In Fig. 1 we show the vector $\mathbf{g} = -g_a(1, 0, 0)^\top$, where g_a is the gravitational acceleration value that is used in the definition of the Rayleigh number Ra, whereas the corresponding vector is in the last term of (3).

In what follows, we omit caps over variables which denote that we consider the class of solutions of form (16).

2. DERIVATION OF THE RESOLVING SYSTEM OF EQUATIONS

In [28], the following relations are obtained for the components of the anisotropy tensor:

$$a_{12}a_{23} - a_{13}a_{22} = 0, \qquad a_{13}a_{23} - a_{12}a_{33} = 0, \qquad a_{23}^2 - a_{22}a_{33} = 0. \tag{26}$$

Owing to (26), rewrite (22) and (23) as

$$\widetilde{K}_I a_{12} = \bar{\tau}_0(A_2 u_y + a_{23}u_z), \qquad \widetilde{K}_I a_{13} = \bar{\tau}_0(A_3 u_z + a_{23}u_y);$$

i.e.,

$$u_y = \mathcal{K}Y a_{12}, \qquad u_z = \mathcal{K}Y a_{13}. \tag{27}$$

Here

$$\widetilde{K}_I = K_I + \beta I, \qquad \mathcal{K} = \frac{W\widetilde{K}_I}{J(1 + W\sigma)}, \qquad \sigma = a_{22} + a_{33}, \qquad I = a_{11} + \sigma.$$

From (24), taking (26) into account, we have

$$a_{23} = -\frac{\beta a_{12}a_{13}}{K_I + \beta\sigma}. \tag{28}$$

Summing up the equations of (21) and taking (26) into account, we obtain

$$K_I\sigma + \beta(\sigma^2 + \mu^2) = 0, \qquad \mu^2 = a_{12}^2 + a_{13}^2. \tag{29}$$

It follows from (28) and (29) that $a_{23} = \sigma a_{12}a_{13}/\mu^2$. Since $a_{22}a_{33} = a_{23}^2$ and $a_{22} + a_{33} = \sigma$, we find

$$a_{22} = \sigma a_{12}^2/\mu^2, \qquad a_{33} = \sigma a_{13}^2/\mu^2. \tag{30}$$

Subtracting (29) from (20) and assuming that $\widetilde{K}_I \neq 0$, we have

$$a_{11} = \sigma + \frac{2W\mu^2}{1 + W\sigma}, \qquad I = 2\left(\sigma + \frac{W\mu^2}{1 + W\sigma}\right). \tag{31}$$

Finally, using (27) and the expressions for $\bar{\tau}_0$, we arrive at the nonlinear equation to determine μ:

$$\widetilde{\mathcal{K}}(\mu^2)\mu = \Lambda := \bar{\tau}_0\lambda, \tag{32}$$

where

$$\lambda^2 = u_y^2 + u_z^2, \qquad \widetilde{\mathcal{K}}(\mu^2) = \mathcal{K}(\mu^2)J = \frac{W\widetilde{K}_I(\mu^2)}{1 + W\sigma(\mu^2)}.$$

Thus, to determine $\mu(\Lambda)$ from (32) we must firstly to find the solutions $\sigma(\mu^2)$ of nonlinear equation (29). Some study of these solutions is presented below, but first we formulate a boundary value problem with respect to the flow velocity u in the channel with rectangular cross section (see Fig. 1).

In view of (27), it follows from (17) that

$$(Ju_y/\widetilde{\mathcal{K}})_y + (Ju_z/\widetilde{\mathcal{K}})_z = -D. \tag{33}$$

Relation (32) determines $\mu = \mu(\Lambda)$. Hence, rewriting (33) by analogy with [28], we formulate the boundary value problem for u:

$$\hat{a}u_{yy} - 2\hat{b}u_{yz} + \hat{c}u_{zz} + \hat{d}u_y + \hat{e}u_z = -D\widetilde{\mathcal{K}}, \qquad u = 0 \ \text{ for } (y,z) \in \partial\Omega, \tag{34}$$

where

$$\hat{a} = 1 - u_y^2\mathcal{L}, \qquad \hat{c} = 1 - u_z^2\mathcal{L}, \qquad \hat{b} = u_yu_z\mathcal{L},$$

$$\hat{d} = (1 - \Delta)\frac{Y_y}{Y} - \Delta\overline{E}_A\frac{Y_y}{Y^2}, \qquad \hat{e} = (1 - \Delta)\frac{Y_z}{Y} - \Delta\overline{E}_A\frac{Y_z}{Y^2},$$

$$\mathcal{L} = \frac{1 - \Delta}{\lambda^2}, \qquad \Delta = \frac{\Lambda}{\mu}\mu_\Lambda.$$

Differentiating (32) with respect to Λ, using (31) and the expressions for $\widetilde{\mathcal{K}}$, we find

$$\mu_\Lambda = \frac{1}{\widetilde{\mathcal{K}}_\mu\mu + \widetilde{\mathcal{K}}}, \qquad \widetilde{\mathcal{K}} = \frac{1 + W\sigma + 2W(\bar{k}/3 + \beta)(\sigma(1 + W\sigma) + W\mu^2)}{(1 + W\sigma)^2},$$

$$\widetilde{\mathcal{K}}_\mu = \frac{W\sigma_\mu}{(1 + W\sigma)^2}\left[2(\bar{k}/3 + \beta) - 1\right] + \frac{4W^2\mu}{(1 + W\sigma)^3}(\bar{k}/3 + \beta)\left[W\sigma - W\mu\sigma_\mu + 1\right].$$

Here the function $\sigma = \sigma(\mu^2)$ can have three branches (the specific expressions are given below). Inserting the expressions of these branches into the expression for $\widetilde{\mathcal{K}}$, and the latter, in turn, into (32), we can compose a cumbersome nonlinear equation for writing the function μ in terms of Λ. In the analytical form, this equation cannot be solved. However, if the solution to the nonlinear equation (34) is sought numerically by some iterative method then it is natural to use (32) for the expression $\mu^{[n]}$ at the nth iteration:

$$\mu^{[n]} = \frac{\bar{\tau}_0\lambda}{\widetilde{\mathcal{K}}\left((\mu^{[n-1]})^2\right)}. \tag{35}$$

Problem (34) should be supplemented by the boundary value problems for the temperature and magnetic field. Taking into account (25)–(27), we obtain

$$\Delta_{y,z}Y + AY\lambda\mu = 0. \tag{36}$$

The equation for L remains the same (see (19)). The boundary conditions for these equations will be formulated in the next section.

After calculating the distributions $u(y,z)$, $Y(y,z)$, and $L(y,z)$, from equations (27), (30), and (31) together with $a_{23} = \sigma a_{12}a_{13}/\mu^2$, we find the distributions of the components of the anisotropy tensor Π; and finally the pressure distribution is obtained using (18).

3. ANALYSIS OF THE MULTIPLICITY OF THE SOLUTIONS OF PROBLEM (34)

We now come back to search for solutions $\sigma(\mu^2)$ of (29) appearing in the formulas for $\widetilde{\mathcal{K}}$ and $\widetilde{\mathcal{K}}_\mu$. Inserting the expressions for K_I in (29) and taking $\sigma = a_{22} + a_{33}$ into account, after some transformations we arrive at the third degree equation

$$a\sigma^3 + b\sigma^2 + c\sigma + d = 0, \qquad \sigma \neq -1/W, \tag{37}$$

$$a = \tilde{\beta}W, \quad b = \tilde{\beta} + 1, \quad c = W^{-1} + W\mu^2\tilde{\beta}, \quad d = \beta\mu^2, \quad \tilde{\beta} = 2\bar{k}/3 + \beta.$$

Following the Cardano formulas for solution of a cubic equation, we introduce the notations

$$p = \frac{3ac - b^2}{3a^2}, \qquad q = \frac{2b^3 - 9abc + 27a^2d}{27a^3}, \qquad \mathcal{Q} = (p/3)^3 + (q/2)^2.$$

After transformations we have $p = \mu^2 - \mathcal{A}$ and $q = \mathcal{B}\mu^2 + \mathcal{C}$, where

$$\mathcal{A} = \frac{1 - \tilde{\beta} + \tilde{\beta}^2}{3\tilde{\beta}^2 W^2}, \qquad \mathcal{B} = \frac{3\beta - \tilde{\beta} - 1}{3W\tilde{\beta}}, \qquad \mathcal{C} = \frac{(1 + \tilde{\beta})(\tilde{\beta} - 2)(2\tilde{\beta} - 1)}{27W^3\tilde{\beta}^3}.$$

In what follows, we will be interested only in the real roots of (37).

For $\mathcal{Q} > 0$ we have the single real root

$$\sigma_1 = \sqrt[3]{-q/2 + \sqrt{\mathcal{Q}}} + \sqrt[3]{-q/2 - \sqrt{\mathcal{Q}}} - b/3a;$$

for $\mathcal{Q} = 0$; the two roots

$$\sigma_1 = -\sqrt[3]{4q} - b/3a, \qquad \sigma_2 = \sqrt[3]{q/2} - b/3a;$$

and for $\mathcal{Q} < 0$; the three real roots

$$\sigma_1 = -2\cos\alpha\,|\sqrt[6]{q^2/4 - \mathcal{Q}}| - b/(3a); \qquad \sigma_{2,3} = -|\sqrt[6]{q^2/4 - \mathcal{Q}}|(-\cos\alpha \pm \sqrt{3}\sin\alpha) - b/(3a),$$

$$\alpha = \arctan(2\sqrt{-\mathcal{Q}}/q)/3.$$

Here and below, the absolute value signs are included to fulfill the condition of continuous dependence of the roots of (37) on $\mathcal{Q}$ in the neighborhood of the point $\mathcal{Q} = 0$.

In the first case, it is easy to calculate that

$$\frac{\partial\sigma_1}{\partial\mu} = \sigma_1' = \frac{(\mathcal{Q}'/\sqrt{\mathcal{Q}} - q')(\sqrt{\mathcal{Q}} + q/2)^{2/3} - (\mathcal{Q}'/\sqrt{\mathcal{Q}} + q')(\sqrt{\mathcal{Q}} - q/2)^{2/3}}{6(\mathcal{Q} - q^2/4)^{2/3}}.$$

In the third case,

$$\frac{\partial\sigma_1}{\partial\mu} = \sigma_1' = \frac{-2^{2/3}}{3\sqrt{-\mathcal{Q}}\,|(q^2 - 4\mathcal{Q})^{5/6}|}\big((q\sin\alpha - 2\sqrt{-\mathcal{Q}}\cos\alpha)\mathcal{Q}' + (q\sqrt{-\mathcal{Q}}\cos\alpha - 2\mathcal{Q}\sin\alpha)q'\big).$$

Next,

$$\frac{\partial\sigma_{2,3}}{\partial\mu} = \sigma_{2,3}' = \frac{-1}{3\sqrt[3]{2}\sqrt{-\mathcal{Q}}\,|(q^2 - 4\mathcal{Q})^{5/6}|}\big(\pm(\sqrt{3}\cos\alpha \pm \sin\alpha)(2\mathcal{Q}q' - q\mathcal{Q}')$$

$$+ (\cos\alpha \mp \sqrt{3}\sin\alpha)(2\mathcal{Q}' - qq')\sqrt{-\mathcal{Q}}\big),$$

where for σ_2 we choose the upper sign from $\pm$ and $\mp$; while for σ_3, the lower sign;

$$q' = \frac{\partial q}{\partial\mu} = -2\mu\frac{1 - 3\beta + \tilde{\beta}}{3\tilde{\beta}W},$$

$$\mathcal{Q}' = \frac{\partial\mathcal{Q}}{\partial\mu} = \frac{\mu}{27\tilde{\beta}^4W^4}\big\{27\beta^2\tilde{\beta}^2\mu^2W^2 + \tilde{\beta}\big(1 + \tilde{\beta}\mu^2W^2\big)\big[\tilde{\beta}(\tilde{\beta}(6\mu^2W^2 - 1) + 4) - 1\big]$$

$$- \beta(1 + \tilde{\beta})\big[\tilde{\beta}\big(2\tilde{\beta}(9\mu^2W^2 - 1) + 5\big) - 2\big]\big\}.$$

In order to determine which of the indicated three options is realized, we denote $\mathcal{M} = \mu^2 \geqslant 0$ and consider the function

$$\mathcal{Q}(\mathcal{M}) = 1/27\,\mathcal{M}^3 + (\mathcal{B}^2/4 - \mathcal{A}/9)\mathcal{M}^2 + (\mathcal{A}^2/9 + \mathcal{B}\mathcal{C}/2)\mathcal{M} + (\mathcal{C}^2/4 - \mathcal{A}^3/27).$$

The roots $\mathcal{M}_1$, $\mathcal{M}_2$, and $\mathcal{M}_3$ of equation $\mathcal{Q}(\mathcal{M}) = 0$ can also be determined using the Cardano formulas. The number of real roots and their positions determine the domains of positive and negative $\mathcal{Q}$, i.e., the number of solutions to the original equation (37). Using the expression for the discriminant $\tilde{\Delta}$ of the equation $\mathcal{Q}(\mathcal{M}) = 0$, we can calculate how many real roots this equation has. Here

$$\tilde{\Delta} = \frac{a_1 a_2 a_3 a_4^3}{2^4 3^{12} \tilde{\beta}^{12} W^{12}}, \quad a_1 = \beta, \quad a_2 = 2\bar{k}/3, \quad a_3 = \beta - 1, \quad a_4 = (1 + \tilde{\beta})^3 - 9\beta(1 + (\tilde{\beta} - 1)\tilde{\beta}).$$

Remark 5. The inequality $\tilde{\Delta} < 0$ means that

$$\mathcal{M}_1 \in \mathbb{R}, \qquad \mathcal{M}_2 = \overline{\mathcal{M}_3} \in \mathbb{C}.$$

Hereinafter, it is used that $\mathcal{M}_2\mathcal{M}_3 \in \mathbb{R}$ and $\mathcal{M}_2\mathcal{M}_3 \geqslant 0$. The equality $\tilde{\Delta} = 0$ means that the roots $\mathcal{M}_1, \mathcal{M}_2, \mathcal{M}_3 \in \mathbb{R}$ and two of these coincide. The inequality $\tilde{\Delta} > 0$ means that $\mathcal{M}_1, \mathcal{M}_2, \mathcal{M}_3 \in \mathbb{R}$. Next, for such $\tilde{\Delta}$ we assume that $\mathcal{M}_1 < \mathcal{M}_2 < \mathcal{M}_3$.

We arrive at the following cases:

Case 1. Equation (37) has a unique solution at all points of Ω if (1) $\tilde{\Delta} < 0$ and $\mathcal{M}_1 < 0$ or (2) $\tilde{\Delta} \geqslant 0$ and $\mathcal{M}_1 \leqslant \mathcal{M}_2 \leqslant \mathcal{M}_3 < 0$.

Case 2. Equation (37) has a unique solution at those points of Ω, where μ is sufficiently small $(0 \leqslant \mu^2 < \mathcal{M}_2)$ or sufficiently large $(\mu^2 > \mathcal{M}_3)$, and nonunique solution at all other points if $\tilde{\Delta} \geqslant 0$ and $\mathcal{M}_1 \leqslant 0 < \mathcal{M}_2 \leqslant \mathcal{M}_3$.

Case 3. Equation (37) has different solutions at those points Ω where $0 \leqslant \mu^2 \leqslant \mathcal{M}_1$ (μ is sufficiently small) or $\mathcal{M}_2 \leqslant \mu^2 \leqslant \mathcal{M}_3$, and a unique solution at other points if (1) $\tilde{\Delta} < 0$ and $\mathcal{M}_1 > 0$ or (2) $\tilde{\Delta} \geqslant 0$ and $0 < \mathcal{M}_1 \leqslant \mathcal{M}_2 \leqslant \mathcal{M}_3$.

Case 4. Equation (37) has different solutions at those points of Ω where μ is sufficiently small $(0 \leqslant \mu^2 \leqslant \mathcal{M}_3)$ and a unique solution at the remaining points if $\tilde{\Delta} \geqslant 0$ and $\mathcal{M}_1 \leqslant \mathcal{M}_2 \leqslant 0 < \mathcal{M}_3$.

Let us note first that $\mathcal{Q}(\mathcal{M}) \to \infty$ as $\mathcal{M} \to \infty$. Secondly, due to no-slip conditions on the channel walls, in the vicinity of the corners of the rectangular channel Ω, the velocity u, its derivatives, and, thus, the values of λ are close to zero. The only physically correct solution to equation (32) for $\lambda = 0$ is $\mu = 0$. Thus, under the assumption of continuity of the components of the stress tensor, there are points in the domain of the solution to the problem with the values $\mu = \sqrt{a_{12}^2 + a_{13}^2}$ that are arbitrarily close to zero.

Taking into account the inequalities of Cases 1−4 and the Vieta formulas for the solutions of the third degree equation, we arrive at the conditions for determining the right-hand side and the coefficients of boundary value problem (34).

In what follows, the above-described numbering of Cases 1−4 for (37) is preserved, but now these statements will be formulated for the right-hand side and coefficients of (34):

Case 1′. The right-hand side and coefficients of (34) are uniquely determined if (1) $\tilde{\Delta} < 0$ and $\mathcal{M}_1\mathcal{M}_2\mathcal{M}_3 = \mathcal{A}^3 - 27\mathcal{C}^2/4 < 0$ or (2) $\tilde{\Delta} \geqslant 0$ and

$$\mathcal{M}_1 + \mathcal{M}_2 + \mathcal{M}_3 = 3\mathcal{A} - 27\mathcal{B}^2/4 < 0,$$

$$\mathcal{M}_1\mathcal{M}_2 + \mathcal{M}_1\mathcal{M}_3 + \mathcal{M}_2\mathcal{M}_3 = 3\mathcal{A}^2 + 27\mathcal{B}\mathcal{C}/2 > 0, \qquad \mathcal{M}_1\mathcal{M}_2\mathcal{M}_3 = \mathcal{A}^3 - 27\mathcal{C}^2/4 < 0.$$

Case 2′. The right-hand side and coefficients of (34) are uniquely determined in the class of continuous functions but can have infinitely many values in the class of discontinuous functions if $\tilde{\Delta} \geqslant 0$ and $\mathcal{M}_1\mathcal{M}_2\mathcal{M}_3 = \mathcal{A}^3 - 27\mathcal{C}^2/4 \leqslant 0$ and, in this case, either

$$\mathcal{M}_1 + \mathcal{M}_2 + \mathcal{M}_3 = 3\mathcal{A} - 27\mathcal{B}^2/4 \geqslant 0,$$

or

$$\mathcal{M}_1\mathcal{M}_2 + \mathcal{M}_1\mathcal{M}_3 + \mathcal{M}_2\mathcal{M}_3 = 3\mathcal{A}^2 + 27\mathcal{B}\mathcal{C}/2 < 0.$$

Let us comment on this case. If the values of λ at all points of Ω are so small that μ are in the neighborhood of the zero solution of (32), $\mu^2 < \mathcal{M}_2$, then the right-hand side and coefficients of (34) are uniquely determined by expression of $\sigma_1(\mu^2)$. Otherwise, there appear some points in the region Ω, where each of $\sigma_i(\mu^2)$, $i = 1, 2, 3$, can be used to determine the right-hand side and coefficients; and then we have infinitely many variants to determine the coefficients and right-hand side of (34) in the class of discontinuous functions (problem with a multivalued operator) and the only variant in the class of continuous functions corresponding to the branch $\sigma_1(\mu^2)$.

Case 3′. The right-hand side and coefficients of (34) are not uniquely defined both in the class of continuous and discontinuous functions if

$$\mathcal{M}_1\mathcal{M}_2\mathcal{M}_3 = \mathcal{A}^3 - 27\mathcal{C}^2/4 > 0$$

and, in this case, either $\tilde{\Delta} < 0$, or

$$\mathcal{M}_1 + \mathcal{M}_2 + \mathcal{M}_3 = 3\mathcal{A} - 27\mathcal{B}^2/4 > 0, \quad \mathcal{M}_1\mathcal{M}_2 + \mathcal{M}_1\mathcal{M}_3 + \mathcal{M}_2\mathcal{M}_3 = 3\mathcal{A}^2 + 27\mathcal{B}\mathcal{C}/2 > 0.$$

In this case, for sufficiently small λ there are the three different variants for setting the continuous right-hand side and coefficients of (34) using the values of $\sigma_i(\mu^2)$, $i = 1, 2, 3$. If at some point of Ω the values of λ turn out to be greater than some threshold value λ^* (this fact is related to the inequality $\mu^2 > \mathcal{M}_1$); then the right-hand side and coefficients of (34) in the neighborhood of this point are uniquely determined by $\sigma_1(\mu^2)$.

Owing to the fact that, in the domain Ω, there are always points with $\mathcal{M}$ arbitrarily close to 0, the set of values of the differential operator of (34) has the cardinality of continuum.

Let us also note that, with the fixed temperature distribution $Y(y, z)$, the value λ^* corresponds to some threshold value of the pressure gradient $\hat{A}^*$ above which the velocity gradients become large enough; so that the solution μ of (32) is at sufficient distance from the zero solution of the same equation for $\lambda = 0$; more precisely, at some distance greater than $\sqrt{\mathcal{M}_1}$. From this it is easy to conclude that, for $\hat{A} < \hat{A}^*$, there are the three options in the class of continuous functions for obtaining the resolving equation (34), whereas for $\hat{A} > \hat{A}^*$, there is the only option.

Case 4′. The right-hand side and the coefficients of equation (34) are determined nonuniquely in the classes of continuous and discontinuous functions if

$$\tilde{\Delta} \geqslant 0, \qquad \mathcal{M}_1\mathcal{M}_2\mathcal{M}_3 = \mathcal{A}^3 - 27\mathcal{C}^2/4 \geqslant 0$$

and, in this case, either

$$\mathcal{M}_1 + \mathcal{M}_2 + \mathcal{M}_3 = 3\mathcal{A} - 27\mathcal{B}^2/4 \leqslant 0,$$

or

$$\mathcal{M}_1\mathcal{M}_2 + \mathcal{M}_1\mathcal{M}_3 + \mathcal{M}_2\mathcal{M}_3 = 3\mathcal{A}^2 + 27\mathcal{B}\mathcal{C}/2 < 0.$$

This case is similar to the previous one with the exception that the fact of exceeding the threshold value λ^* is determined by the inequality $\mu^2 > \mathcal{M}_3$.

In the conclusion of studying the set of values of the operator of problem (34) we note that

$$\mathcal{M}_1\mathcal{M}_2\mathcal{M}_3 = \mathcal{A}^3 - \frac{27\mathcal{C}^2}{4} = \frac{(\widetilde{\beta} - 1)^2}{4W^6\widetilde{\beta}^4} \geqslant 0.$$

This means that only the cases 3 or 4 are realized.

Remark 6. Note that the question of uniqueness of solutions of quasilinear elliptic equations is difficult and can be solved only in some special cases. In this study, any rigorous analysis of the existence and uniqueness of solutions to problem (34), (36), (19) when using $\sigma_i(\mu)$, $i = 1, 2, 3$, was not carried

out. However, in numerical experiments while using σ_1 and σ_3, we succeeded in obtaining two different approximate solutions (see Section 5.1). To understand which of these solutions is realized in practice for the stationary flow of a polymeric fluid, the additional analysis of stability of each obtained solution is needed and, moreover, in the original spatial statement.

Remark 7. For $\bar{k} = 0$, instead of (37) it is not difficult to obtain some quadratic equation for σ. The roots of this equation can be easily found:

$$\sigma = \pm\sqrt{1 - q^2} - 1/(2\widetilde{W}), \qquad q^2 = (2\widetilde{W}\mu)^2 < 1, \qquad \widetilde{W} = \beta W.$$

In this case, the expression for $\mathcal{K}$ has the form

$$\mathcal{K} = \widetilde{\mathcal{K}}/J, \qquad \widetilde{\mathcal{K}} = \frac{2\beta(\rho\sqrt{1-q^2}+1)}{(\rho + \sqrt{1-q^2})^2}, \qquad \rho = 2\beta - 1, \qquad |\rho| < 1.$$

After cumbersome calculations in [28], it is obtained for the case of $\bar{k} = 0$:

$$\Delta = \frac{(1 - \varkappa^2\tilde{t}^2)(1 + \tilde{t}^2)}{Q}, \qquad Q = 1 - \varkappa^2\tilde{t}^4 - \frac{6\rho}{1-\rho}\tilde{t}^2 + 4\Lambda\frac{\tilde{t}(1-\tilde{t}^2)}{1-\rho},$$

where $\tilde{t} = \tilde{g} \pm \sqrt{\tilde{g}^2 - 1}$ and $\tilde{g} > 1$; moreover,

$$\tilde{g} = \frac{1 + \sqrt{1 + 4\Lambda^2}}{2\Lambda}, \qquad \Lambda = \sqrt{1 - \rho^2}W\Lambda, \qquad \varkappa = \sqrt{\frac{1+\rho}{1-\rho}}.$$

In this case,

$$\sigma = -\frac{(\varkappa t)^2}{\beta W(1 + (\varkappa t)^2)}.$$

4. STATEMENT OF BOUNDARY VALUE PROBLEMS IN CHANNELS WITH ELLIPTICAL AND CIRCULAR CROSS-SECTIONS AND HEATING ELEMENTS

4.1. A Channel with Elliptical Cross-Section

Under consideration is the flow in a cylindrical channel $\widetilde{\Omega}$ with an elliptical cross-section and some thin elliptical heating element with the same foci as for the outer boundary of the channel (Fig. 2,a).

It is assumed that the inner wall of the channel (inner ellipse) is made of a substance that is a paramagnetic, for example, aluminum or tungsten, for which the magnetic susceptibility is $\chi_{0H} > 0$. There is a winding on the surface of the inner ellipse so that there are n turns per unit length (1 m in SI). In this case, a magnetic field appears inside the channel with a single nonzero component of the intensity vector L (see (16)).

Let us write problem (34) in the elliptic coordinates α and γ:

$$y = \delta\cosh\alpha\sin\gamma, \qquad z = \delta\sinh\alpha\cos\gamma, \tag{38}$$

where $\delta = \sqrt{1 - r_1^2}$ (2δ is the focal length), $0 \leqslant \alpha < \infty$, and $0 \leqslant \gamma \leqslant 2\pi$. Owing to (38), we have

$$y_\alpha = -z_\gamma = \delta\sinh\alpha\sin\gamma, \qquad z_\alpha = y_\gamma = \delta\cosh\alpha\cos\gamma, \qquad y_{\alpha\alpha} = -y_{\gamma\gamma} = y, \qquad y_{\alpha\gamma} = z. \tag{39}$$

$$u_y = Ru_\alpha + Qu_\gamma, \qquad u_z = Qu_\alpha - Ru_\gamma. \tag{40}$$

Here

$$R = \frac{y_\alpha}{y_\alpha^2 + y_\gamma^2} = \frac{\delta\sinh\alpha\sin\gamma}{g^2}, \qquad Q = \frac{y_\gamma}{y_\alpha^2 + y_\gamma^2} = \frac{\delta\cosh\alpha\cos\gamma}{g^2}, \qquad g^2 = \delta^2(\sinh^2\alpha + \cos^2\gamma).$$

By (40), we obtain

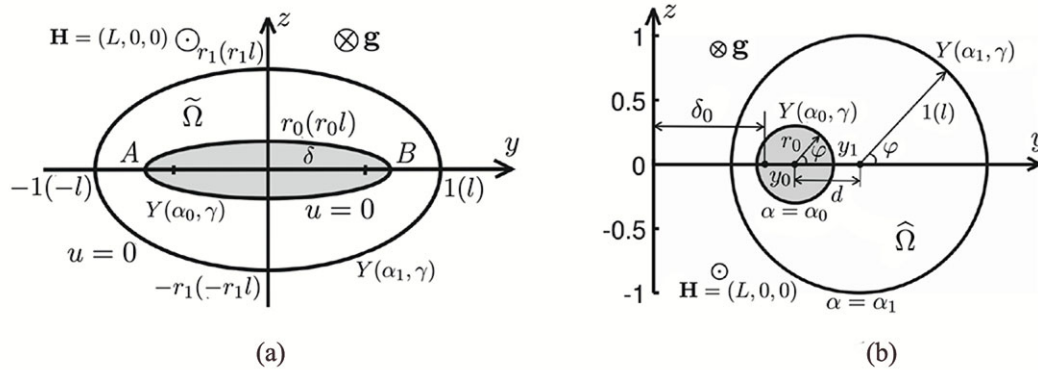$$\lambda^2 = u_y^2 + u_z^2 = \frac{1}{g^2}\left(u_\alpha^2 + u_\gamma^2\right). \tag{41}$$

Fig. 2. Cross-sections of an elliptical channel with a heating element (a) and a channel formed by two cylinders with distance d between the axes (b).

Taking (40) into account, we successively infer

$$u_{yy} = R^2 u_{\alpha\alpha} + 2RQ u_{\alpha\gamma} + Q^2 u_{\gamma\gamma} + (RR_\alpha + QR_\gamma)u_\alpha + (RQ_\alpha + QQ_\gamma)u_\gamma,$$

$$u_{zz} = Q^2 u_{\alpha\alpha} - 2RQ u_{\alpha\gamma} + R^2 u_{\gamma\gamma} + (QQ_\alpha - RQ_\gamma)u_\alpha + (RR_\gamma - QR_\alpha)u_\gamma,$$

$$(42)$$

whereas

$$R_\alpha = Q_\gamma = \frac{\delta^2 y(\cos^2\gamma - \sinh^2\alpha)}{g^4}, \qquad R_\gamma = -Q_\alpha = \frac{\delta^2 z(\cosh^2\alpha + \sin^2\gamma)}{g^4}.$$

By analogy, we find

$$u_{yz} = RQ u_{\alpha\alpha} + (Q^2 - R^2)u_{\alpha\gamma} - RQ u_{\gamma\gamma} + (RQ_\alpha + QQ_\gamma)u_\alpha - (RR_\alpha + QR_\gamma)u_\gamma. \qquad (43)$$

In view of (42) and (43), quasilinear equation (34) assumes the following form:

$$\tilde{a} u_{\alpha\alpha} - 2\tilde{b} u_{\alpha\gamma} + \tilde{c} u_{\gamma\gamma} + \tilde{d} u_\alpha + \tilde{e} u_\gamma = D\widetilde{\mathcal{K}}, \qquad (44)$$

where

$$\tilde{a} = \hat{a}R^2 + \hat{c}Q^2 - 2\hat{b}RQ = \frac{1}{g^2} - \frac{u_\alpha^2}{g^4}\mathcal{L}, \qquad \tilde{c} = \hat{a}Q^2 + \hat{c}R^2 + 2\hat{b}RQ = \frac{1}{g^2} - \frac{u_\gamma^2}{g^4}\mathcal{L},$$

$$\tilde{b} = \hat{b}(Q^2 - R^2) + RQ(\hat{c} - \hat{a}) = \frac{u_\alpha u_\gamma}{g^4}\mathcal{L},$$

$$\tilde{d} = (\hat{a} - \hat{c})(RR_\alpha + QR_\gamma) - 2\hat{b}(QR_\alpha - RR_\gamma) + R\hat{d} + Q\hat{e}$$

$$= \frac{\mathcal{L}}{g^2}[(R_\gamma Q - R_\alpha R)(u_\alpha^2 - u_\gamma^2) - 2(R_\gamma R + R_\alpha Q)u_\alpha u_\gamma] + \frac{(1-\Delta)Y - \Delta}{(Yg)^2}Y_\alpha,$$

$$\tilde{e} = (\hat{a} - \hat{c})(QR_\alpha - RR_\gamma) + 2\hat{b}(RR_\alpha + QR_\gamma) + Q\hat{d} - R\hat{e}$$

$$= \frac{\mathcal{L}}{g^2}[(R_\gamma R + R_\alpha Q)(u_\alpha^2 - u_\gamma^2) + 2(R_\gamma Q - R_\alpha R)u_\alpha u_\gamma] + \frac{(1-\Delta)Y - \Delta}{(Yg)^2}Y_\gamma,$$

whereas

$$R_\gamma Q - R_\alpha R = \frac{\delta^2}{g^4}\sinh\alpha\cosh\alpha, \qquad R_\gamma R + R_\alpha Q = \frac{\delta^2}{g^4}\sin\gamma\cos\gamma.$$

Equation (44) must be supplemented by the heat equation (it is derived from (36) on the basis of the change of coordinates (38) and formulas (39)–(41)):

$$Y_{\alpha\alpha} + Y_{\gamma\gamma} + \left(Ag\mu\sqrt{u_\alpha^2 + u_\gamma^2}\right)Y = 0. \qquad (45)$$

The equation for L takes the form

$$L_{\alpha\alpha} + L_{\gamma\gamma} = 0. \tag{46}$$

The domain of (44)–(46) is located between the confocal ellipses with small semiaxes $r_0 < r_1$ (see Fig. 2, a); therefore, $\alpha_0 \leqslant \alpha \leqslant \alpha_1$ and, by (38),

$$\alpha_{0,1} = \frac{1}{2} \ln\left(\frac{1 + r_{0,1}}{1 - r_{0,1}}\right).$$

Thus, we will look for solutions of equation (44)–(46) in the class of sufficiently smooth functions which are 2π-periodic with respect to the variable γ and satisfy no-slip conditions for the velocity on the channel walls

$$u = 0 \quad \text{for } \alpha = \alpha_0, \alpha_1 \tag{47}$$

and inhomogeneous Dirichlet conditions for temperature and magnetic field

$$Y(\alpha_0, \gamma) = \psi_0^Y(\gamma), \qquad Y(\alpha_1, \gamma) = \psi_1^Y(\gamma), \tag{48}$$

$$L(\alpha_0, \gamma) = \psi_0^L(\gamma), \qquad L(\alpha_1, \gamma) = \psi_1^L(\gamma). \tag{49}$$

Here $\psi_{0,1}^{Y,L}(\gamma)$ are the given temperature and magnetic field distributions on the inner and outer walls. When the current I_H is passed along the winding of the inner channel, we have in accordance with [25, 26, 30] $\psi_0^L(\gamma) \equiv nI_H/H_0$ (here H_0 is the characteristic value of intensity for nondimensionalization). Under the assumption that the channel is in an external magnetic field that is codirectional with the axis of the channel and of intensity $\mathbf{H_0} = (L_0(\alpha, \gamma), 0, 0)$, while the outer wall of the channel has a small thickness; we obtain $\psi_1^L(\gamma) = L_0(\alpha_1, \gamma)$. Using the Curie Law (see [25, 26, 30, 31]) it is possible to express the temperature on the inner wall through its magnetization m:

$$\psi_0^Y(\gamma) \equiv \chi_{H0} nI_H/m$$

(see Remark 1). The function $\psi_1^Y(\gamma)$ is determined by the external temperature field. In our calculations,

$$\psi_1^Y(\gamma) \equiv T_0/T_0 = 1.$$

Note that for small values of r_0 at the points $\alpha = r_0$, $\gamma = \pi/2$ and $\alpha = r_0$, $\gamma = 3\pi/2$ (points A and B in Fig. 2, a) the function g in the denominators of the coefficients of (44) takes small values. If we multiply (44) by g^6 then we arrive at an equation with a small parameter g^2 at the higher derivatives. It means that, in the vicinity of these points, the solutions to this equation can have essential singularities.

Remark 8. Note that, according to the reasoning in Section 3 and owing to the smoothness of the boundary of the channel under study, the minimum values of λ and μ can be arbitrarily large, but they, as before, are proportional to the pressure gradient. For small gradients, λ and μ are small; and so, in the class of continuous functions there are the three possible options for writing equation (44), which correspond to σ_1, σ_2, and σ_3. As pressure increases (when points with positive and negative values of $\mathcal{Q}$ appear in the region Ω), the only one option remains of writing (44) with continuous coefficients and right-hand side but an infinite set of options in the class of discontinuous functions. With further increase in the pressure gradient, the values of $\mathcal{Q}$ become positive throughout Ω; then there remains a unique option of writing (44) both in the classes of smooth and discontinuous functions.

4.2. A Channel with Circular Cross-Section

Let us pose a problem concerning the polymeric fluid flow in a channel $\widehat{\Omega}$ formed by two cylinders of radii $0 < r_0 < 1$ and $r_1 = 1$ with parallel axes spaced at distance d, $0 \leqslant d < 1 - r_0$. In Fig. 2 b, the cross-section of the channel is shown. As in the above case, we assume that the inner wall of the channel (in this case, the cylinder) is wrapped with some thin wiring with n turns per unit length that passes the current of strength I_H.

In (34) we make the change to the bipolar coordinate system. Within the scope of this subsection, we denote the bipolar coordinates by (α, γ) so that

$$y = \delta_0 \frac{\sinh \alpha}{\cosh \alpha - \cos \gamma}, \qquad z = \delta_0 \frac{\sin \gamma}{\cosh \alpha - \cos \gamma},$$

$$\delta_0 = 1 - r_0^2/\nu, \qquad \nu = \sqrt{d^2(1 + r_0^2) + 2d\omega}, \qquad \omega = \sqrt{(1 - r_0^2)^2 + (dr_0)^2}, \qquad (50)$$

$$0 \leqslant \alpha < \infty, \qquad 0 \leqslant \gamma \leqslant 2\pi.$$

After calculations, as in Section 4.1, for the temperature rate and the component L of the magnetic field intensity, we obtain equations of the form (44)–(46) with the same expressions for the coefficients $\tilde{a}$–$\tilde{e}$ but with the following changes: δ should be replaced with δ_0 and some items should be calculated as follows:

$$y_\alpha = -z_\gamma = \delta_0 \frac{1 - \cos \gamma \cosh \alpha}{(\cos \gamma - \cosh \alpha)^2}, \qquad y_\gamma = z_\alpha = \delta_0 \frac{\sin \gamma \sinh \alpha}{(\cos \gamma - \cosh \alpha)^2},$$

$$g = \frac{\delta_0}{(\cos \gamma - \cosh \alpha)}, \qquad R = \frac{1 - \cos \gamma \cosh \alpha}{\delta_0}, \qquad Q = -\frac{\sin \gamma \sinh \alpha}{\delta_0},$$

$$R_\alpha = Q_\gamma = -\frac{\cos \gamma \sinh \alpha}{\delta_0}, \qquad R_\gamma = Q_\alpha = \frac{\sin \gamma \cosh \alpha}{\delta_0},$$

$$R_\gamma Q - R_\alpha R = \frac{(\cos \gamma - \cosh \alpha) \sinh \alpha}{\delta_0^2}, \qquad R_\gamma R - R_\alpha Q = \frac{(\cosh \alpha - \cos \gamma) \sin \gamma}{\delta_0^2}.$$

The equations of the circles of radii r_0 and 1 (see Fig. 2, b) in the bipolar coordinate system (50) have the form

$$\alpha = \alpha_0 = \operatorname{arctanh}\left(\frac{dr_0^2 + \omega}{1 - r_0^2}\right), \qquad \alpha = \alpha_1 = \operatorname{arctanh}\left(\frac{d + \omega}{1 - r_0^2}\right),$$

the coordinates of the centers of the circles in the bipolar system are $y_0 = \coth \alpha_0$ and $y_1 = \coth \alpha_1$.

As to the boundary conditions, it is also convenient to have expressions for the coordinates of points of the indicated circles in the bipolar system (α, γ) through the polar coordinates (r, φ) with the pole at $(y_0, 0)$ for the inner circle:

$$\alpha(\varphi) = \operatorname{arctanh}\left(\frac{2(1 - r_0^2)(y_0 + r_0 \cos \varphi)}{(r_0^2 + 2r_0 y_0 \cos \varphi + y_0^2)\nu + (1 - r_0^2)^2/\nu}\right),$$

$$\gamma(\varphi) = \arctan\left(\frac{2r_0(1 - r_0^2) \sin \varphi}{(r_0^2 + 2r_0 y_0 \cos \varphi + y_0^2)\nu - (1 - r_0^2)^2/\nu}\right)$$

and the pole at $(y_1, 0)$ for the outer circle:

$$\alpha(\varphi) = \operatorname{arctanh}\left(\frac{2(1 - r_0^2)(y_1 + \cos \varphi)}{(1 + 2y_1 \cos \varphi + y_1^2)\nu + (1 - r_0^2)^2/\nu}\right),$$

$$\gamma(\varphi) = \arctan\left(\frac{2(1 - r_0^2) \sin \varphi}{(1 + 2y_1 \cos \varphi + y_1^2)\nu - (1 - r_0^2)^2/\nu}\right).$$

The solutions of (44) in the problem concerning the flow between two cylinders belong to the class of functions which are 2π-periodic in the variable γ and satisfy the Dirichlet conditions:

$$u(\alpha_0, \gamma) = u(\alpha_1, \gamma) = 0;$$

$$Y(\alpha_0, \gamma) = \psi_0^Y(\gamma) = \psi_0^Y(\gamma(\varphi)), \qquad Y(\alpha_1, \gamma) = \psi_1^Y(\gamma) = \psi_1^Y(\gamma(\varphi)),$$

$$L(\alpha_0, \gamma) = \psi_0^L(\gamma) = \psi_0^L(\gamma(\varphi)), \qquad L(\alpha_1, \gamma) = \psi_1^L(\gamma) = \psi_1^L(\gamma(\varphi)),$$
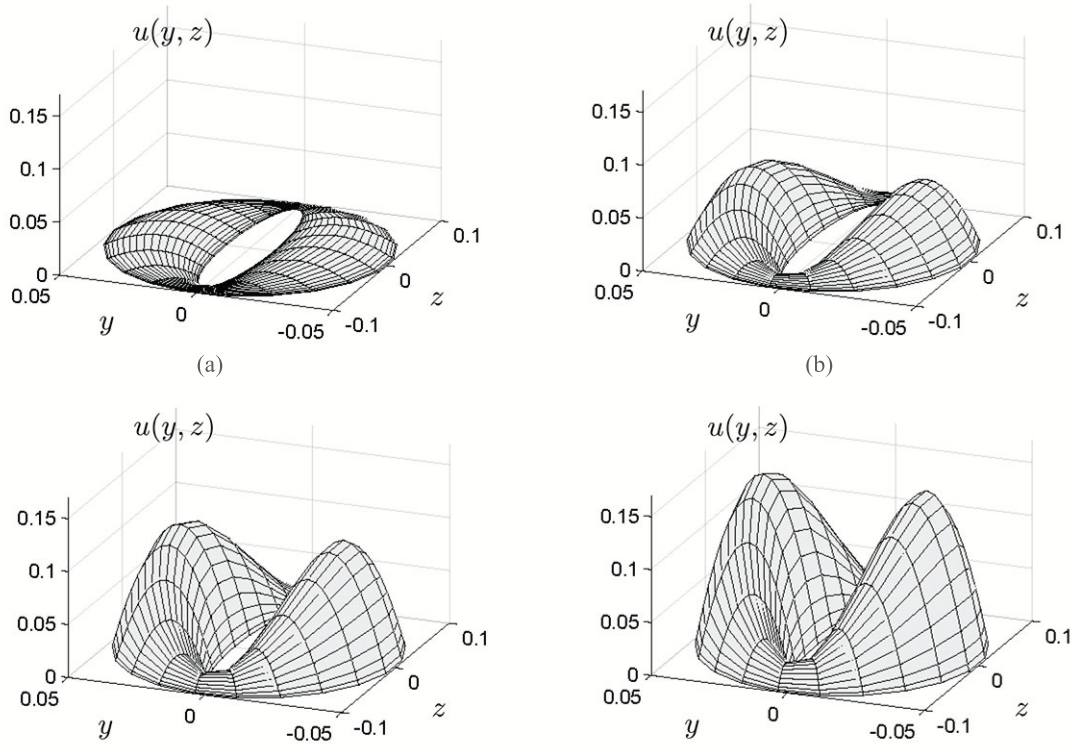
Fig. 3. Distribution of the flow velocity $u(y, z)$ (m/s) in an elliptical nozzle with a heating element at the different values of the pressure gradient in the nozzle: $\widehat{\Delta P} = 0.7$ atm (a), 2.8 (b), 4.8 (c), and 6.9 atm (d).

where $\psi_{0,1}^{Y,L}(\gamma(\varphi))$ are the given temperature and magnetic field distributions with respect to angular coordinates φ on the outer and inner circles. They can be determined by analogy to those in Section 3.

It is easy that for small r_0 the parameter α_0 takes large values; therefore, in a neighborhood of the circle $\alpha = \alpha_0$ the values of the function g are small. Wherein there is a certain nonuniformity of this expression with respect to γ. However, for d close to 0 and r_0 close to 1, the values of g again turn out close to 0 in the entire domain of the problem. As noted in Section 4.1, this circumstance can lead to essential singularities of the solution of (44).

5. NUMERICAL SIMULATION OF POLYMERIC FLUID FLOWS

To solve boundary value problem (44)–(49) in Section 4.1, the nonlocal method without saturation (hereinafter NMWS) is used which is implemented in Java as a computer software package [17]. In the works indicated in the list of references, the reader can find a detailed description of this method [16], estimates of the rate of convergence and the round-off error [18], results of tests of the method in the problems with singularities, as well as numerical justification of the absence of saturation of the method in solving nonlinear boundary value problems for equations of elliptic type [19]. As a result of approximation of unknown functions in (44)–(46) by direct (tensor) product of an interpolation polynomial with Chebyshev nodes with respect to the variable α and a trigonometric polynomial with Dirichlet kernel in the variable γ, using the collocation method and the relaxation method that are implemented within the framework of NMWS, we obtain the numerical solutions of the problem (regarding the use of polynomials with the Dirichlet kernel in the framework of this algorithm, see [16]).

5.1. Flow in a Channel with Elliptical Cross-Section

Fig. 3 shows the distribution of the flow velocity of the polymeric fluid in a channel with elliptical cross-section for various values of the pressure gradient $\widehat{\Delta P}$ in the channel with the parameters
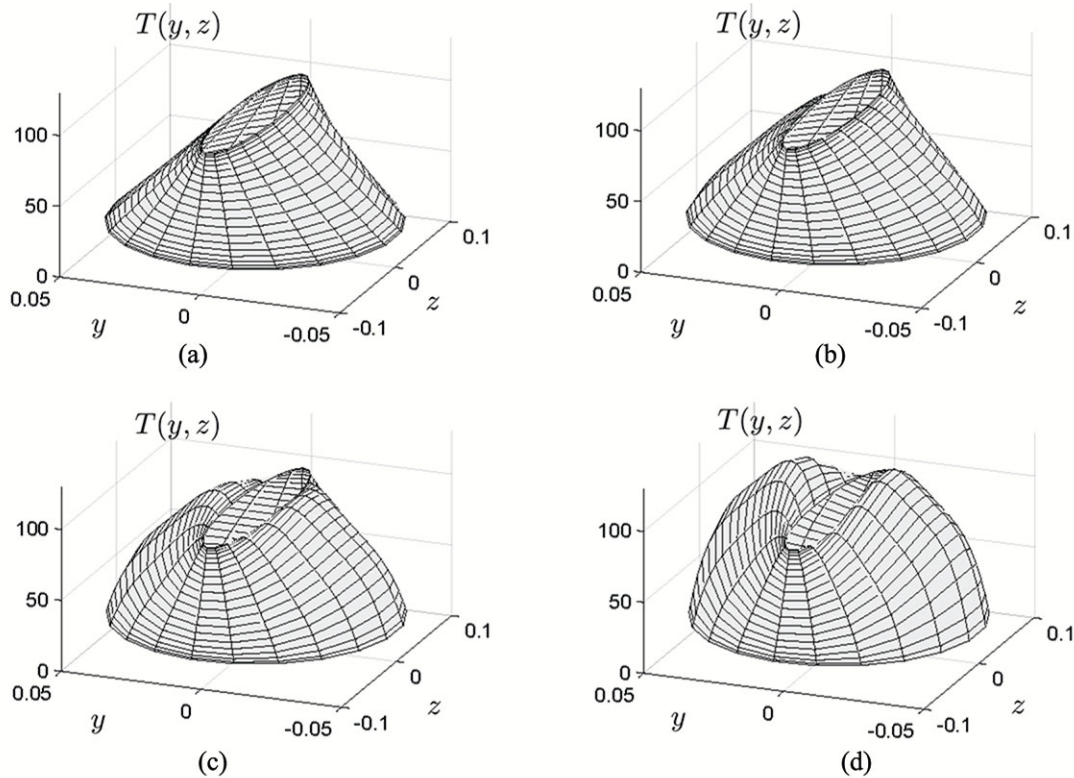
Fig. 4. Distribution of the fluid temperature $T(y,z)$ (°C) in an elliptical nozzle with a heating element at the different values of the pressure gradient in the nozzle: $\widehat{\Delta P} = 0.7$ atm (a), 2.8 (b), 4.8 (c), and 6.9 atm (d).

corresponding to the experimental data in [5−15] (see the Appendix; hereinafter, for convenience, the pressure values are given in atmospheres (atm)).

According to the data from Tables 1 and 2 (see the Appendix), the following values of physical parameters are used:

$$\overline{E}_A = 0.614, \qquad \beta = 0.1, \qquad k = 1.2\beta, \qquad W = 0.1, \qquad H_0 = 1 \text{ A/m},$$
$$n = 22, \qquad I_H = 22 \text{ A}, \qquad m = 0.03 \text{ A/m}, \qquad \chi_{H0} = 7.8 \times 10^{-5}$$

(we assume that the heating element is made of the paramagnet tungsten). The value of the following dissipation coefficient A was not found in the literature; in the calculations, we put it equal to 3. The next values of the geometric parameters were selected: $r_0 = 0.1$ and $r_1 = 0.5$. The degree of tensor product of interpolation polynomials (the number of the spatial grid nodes) was also fixed and equal to 21×21. Note that for given parameter values $\tilde{\Delta} < 0$; i.e. Case 3′ (see Section 3) is realized for the right-hand side and the coefficients of (34), wherein $\mathcal{M}_1 \approx 1882.32$. In Fig. 4, the temperature distribution is given for the operation mode under consideration.

Note that the above values correspond to the solution σ_1 of (37). However, the given values of the pressure gradient are rather small, and there are two more options to write (44) with continuous coefficients and the right-hand side (see Remark 8). Let us note, however, the interesting fact: For the option of using $\sigma_2(\mu^2)$, we cannot find solutions (the relaxation method does not converge with the variation of parameters of the numerical method in wide ranges), while with using $\sigma_3(\mu^2)$ it was possible to find solutions. Cross-sections of the distributions of flow velocity and temperature corresponding to the two branches σ_1 and σ_3 are given in Fig. 5 for the case of $\widehat{\Delta P} = 6.9$ atm. It can be seen that the maximum spread in the values of velocity and temperature for these two branches is large (solutions differ by 5−7 times). In the original spatial statement, to determine a solution realized in practice, additional analysis of the stability of each obtained solution is needed.
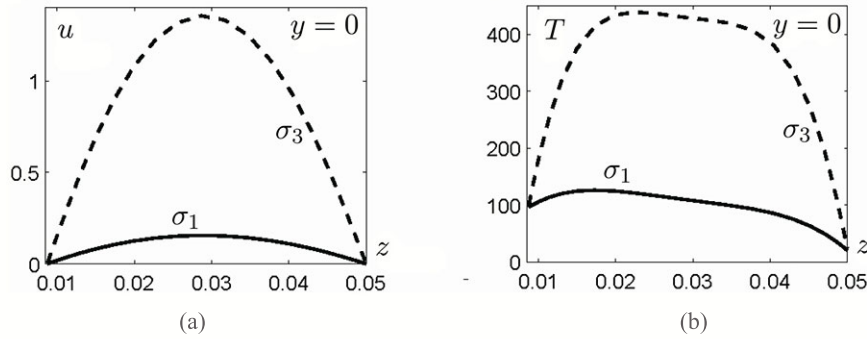
Fig. 5. Section by the plane $y = 0$ of the distribution of the velocity u (m/s) (a) and the temperature T (°C) (b) which correspond to the two different solutions $\sigma = \sigma_1$ and $\sigma = \sigma_3$ of equation (37) with $\widehat{\Delta P} = 6.9$ atm.

Concluding the analysis of the multiplicity of solutions, we note that, for the flow mode under consideration, the threshold pressure gradient value is $\widehat{\Delta P}^* \approx 90$ atm (see Remark 8). For $\widehat{\Delta P} < \widehat{\Delta P}^*$, it is possible to find two solutions with high smoothness; while for $\widehat{\Delta P}^* < \widehat{\Delta P} < \widehat{\Delta P}^{lim} \approx 248$ atm only one smooth solution can be found. With further increase of the pressure gradient, the relaxation method ceases to converge. The indicated threshold and limit values of the gradient $\widehat{\Delta P}^{lim}$ were obtained with accuracy of 1 atm in numerical experiments.

5.2. Flow in a Channel with Circular Cross-Section

Applying NMWS, it was possible to find the approximate solutions to the equations describing nonisothermal magnetohydrodynamic flows of a polymeric fluid between two cylinders (see Section 4.2 and boundary value problem (44)–(49)). By analogy with the reasoning given in Section 5.1, we use the experimental data from Tables 1 and 2 (see the Appendix) and set the following values of the physical parameters:

$$E_A = 0.614, \qquad A = 0.5, \qquad \beta = 0.1, \qquad k = 1.2\beta, \qquad W = 0.1,$$

$$H_0 = 1 \text{ A/m}, \qquad n = 22, \qquad I_H = 22 \text{ A}, \qquad m = 0.03 \text{ A/m}, \qquad \chi_{H0} = 7.8 \times 10^{-5}.$$

The values of the geometric parameters were selected as follows: $r_0 = 0.4$ and $d = 0.2$. The degree of the tensor product of interpolation polynomials was fixed and equal to 31×31. In Fig. 6 the values of the flow velocity are shown for the considered modes.

APPENDIX

IDENTIFICATION OF PARAMETERS OF THE MODEL

We performed the analysis of the available literature sources containing data on the rheological and thermomechanical properties of polymer solutions with different conductivity as well as data on the main parameters of modern technologies of additive manufacturing the products from electrically conductive polymer materials. Based on the obtained data, the values of the main parameters of the above-developed model of the polymeric fluid flow are identified (see Tables 1 and 2).

The rheological properties of polymer solutions and melts include, first of all, the values of shear viscosity and relaxation time, as well as their dependence on shear rates, temperature, and solution concentration. The thermomechanical properties include thermal diffusivity, heat capacity, the coefficient of thermal expansion, and the activation energy. Other properties of interest to researchers include magnetic susceptibility, current-voltage characteristics, maximal charge density, and the electron mobility.
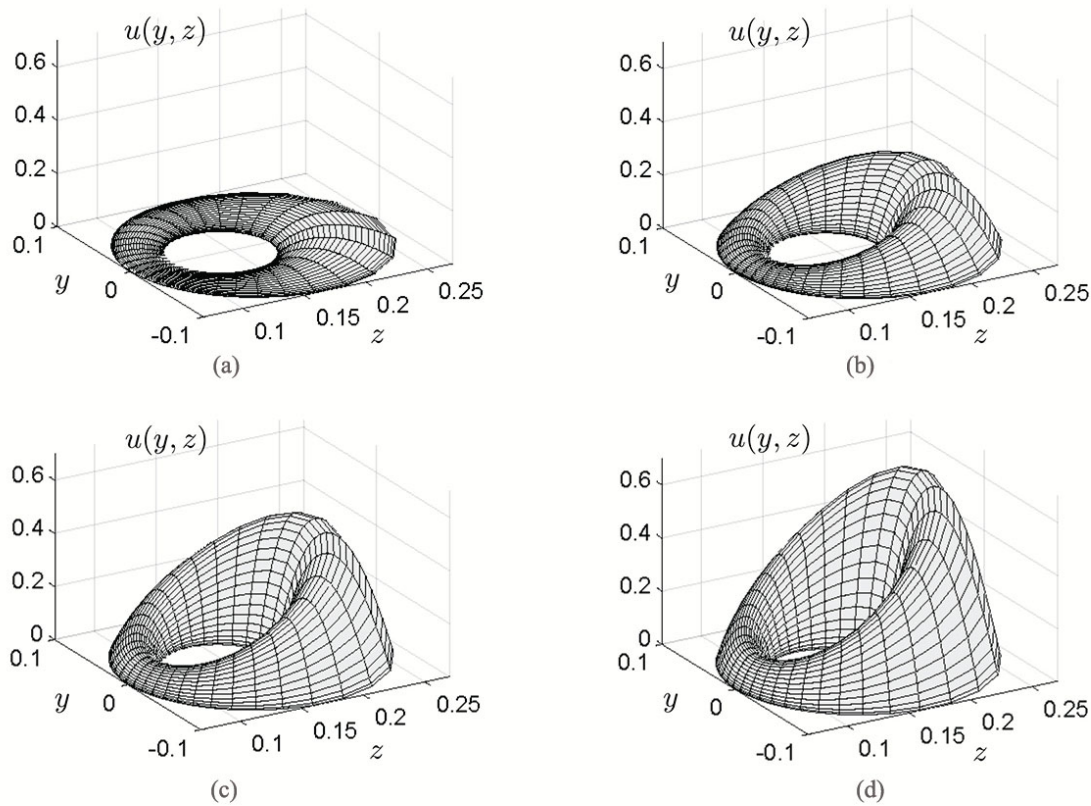
Fig. 6. The flow velocity $u(y, z)$ (m/s) in a cylindrical nozzle with a heating element at the different values of the pressure gradient: $\widehat{\Delta P} = 0.7$ atm (a), 2.8 (b), 4.8 (c), and 6.9 atm (d).

For manufacturing electrically conductive devices, there are used polymer semiconductors such as polyethylene glycol, polyacrylamide, etc., high conductivity polymer materials (the most common is PEDOT:PSS) and polymer-based materials with the impurities of nanoparticles of electrically conductive metals (typically, silver or gold nanoparticles).

In the literature sources, there is also information about the mechanical characteristics of printing devices: the characteristic sizes of nozzles and drops of ink, the values of velocities and fluid flows in the nozzle, maximum resolution in printing, pressure in nozzles, etc. The most common printing technologies are piezoelectric and thermal inkjets.

All indicated data were used to identify the parameters of the above-developed model for calculating the flows of PEDOT:PSS (see Tables 1 and 2). The values of the phenomenological parameters β and $\bar{k}$ of the Pokrovskii−Vinogradov model were investigated in [1, 5]. It was found that for many linear polymers $\beta \in [0, 0.5]$, $\bar{k} = \beta$ or $\bar{k} = 1.2\beta$.

For calculating the Reynolds, Weissenberg, Rayleigh, and Prandtl numbers for the PEDOT: PSS solutions (see Table 3) the following formulas were used:

$$\text{Re} = \frac{\rho u_H l}{\eta_0^*}, \qquad \text{W} = \frac{\tau_0^* u_H}{l}, \qquad \text{Ra} = \frac{g_a b \Delta T l^3 c_P \rho^2}{\eta_0^* c_T}, \qquad \text{Pr} = \frac{\eta_0^* c_P}{c_T},$$

where $\Delta T = 200$ K is the characteristic temperature difference between the walls and the liquid, $g_a = 9.81$ m/s^2 is the gravity acceleration, and $\rho = 1000$ kg/m^3 is the fluid density. To calculate the relative dimensionless pressure gradient $\hat{A}$ (see (16)), it was assumed that the nozzle length is 100 times greater than the characteristic section size l and $h = 100$ (see also Fig. 1).

Table 1. Values of the parameters of model (1)–(11) for calculating a stationary flow in the nozzle of a $3D$ printer

Parameter	Notation in model	Units in SI	Reference	Range of values	Value for calculations
Characteristic flow velocity	u_H	m/s	[6, 7]	0.04–1 m/s; in particular cases 3–5 m/s	1 m/s
Characteristic length (section size)	l	micron	[6]	0.1–250 micron	100 micron
Characteristic temperature	T_0	K	[8]	273–700 K (sintering temperature)	(20 °C)
Characteristic magnetic field intensity	H_0	A/m	—	Calculated by the parameters of induction coils	10^4 A/m
Magnetic Permeability (PEDOT:PSS)	μ	—	[9]	$1 + 2.5 \times 10^{-4}$ $- 1 + 3.7 \times 10^{-4}$	$1 + 3 \times 10^{-4}$
Solution Conductivity PEDOT:PSS	σ_e	1/(Om·m)		$800 - 3 \times 10^4$ 1/(Om·m)	10^4 1/(Om·m)
Initial shear viscosity values of conductive solution PEDOT:PSS	η_0^*	Pa·s	[11, 12]	1.3×10^{-3} -3×10^{-1} Pa·s	10^{-2} Pa·s
Initial values of relaxation time of conductive solution PEDOT:PSS	τ_0^*	s	[7]	6×10^{-6} -1.2×10^{-4} s	10^{-5} s
Dimensionless activation energy	$\overline{E}_A$	—	[13]	0.614–6.14	0.614
Thermal conductivity coefficient (for calculation of Pr and Ra numbers)	c_T	W/(m·K)	[14]	0.3–0.37 W/(m·K)	0.37 W/(m·K)
Specific heat capacity (for calculation of Pr and Ra numbers)	c_P	J/(kg·K)	[14]	2000 (J/(kg·K) (solid polymer) -4180 (J/(kg·K) (aqueous solution of low concentration)	4000 J/(kg·K)
Thermal expansion coefficient (for calculation of Ra number)	b	K^{-1}	[15]	5×10^{-5} K^{-1} (solid polymer) $- 6 \times 10^{-4}$ K^{-1} (aqueous solution of low concentration)	5×10^{-4} K^{-1}

Table 2. Continuation of Table 1

Parameter	Notation in model	Units in SI	Reference	Range of values	Value for calculations
Pressure gradient in the channel	$\widehat{\Delta P}$	Pa	[6, 8]	6.9×10^4 -6.9×10^5 Pa	10^5 Pa
Dimensionless gradient under condition that the nozzle length is 100 times greater than the diameter	$\widehat{A}$	—	[6, 8]	$0.69-6.9$	1
Characteristic of orientation of the macromolecular coil	β	—	[1, 5]	$0-0.5$	0.1
Characteristic of size of the macromolecular coil	$\bar{k}$	—	[1, 5]	$\bar{k} \in [\beta, 1.2\beta]$	$\bar{k} = 1.2\beta$

Table 3. Values of Reynolds, Weissenberg, Rayleigh, and Prandtl numbers for aqueous solutions PEDOT:PSS

Parameter	Notation in the model	Units in SI	Range of values	Value for calculations
Reynolds number	Re	—	10	10
Weissenberg number	W	—	$0.06-1.2$	0.1
Rayleigh number	Ra	—	1.06	1.06
Prandtl number	Pr	—	108.1	108.1

CONCLUSION

We propose the model that describes stationary nonisothermal MHD flows of an incompressible viscoelastic polymeric fluid in the channels with rectangular, elliptical, and circular cross sections.

It is shown that the model allows multiple solutions and actually contains a multi-valued operator, whose range of values consists of finitely many points and is surely not convex. The model parameters are identified according to tests of the materials and devices used in the 3D printing.

We use the non-local algorithm without saturation to search for sufficiently smooth solutions to the problems posed and analyze their multiplicity.

Two different solutions were found for the flow regime under consideration. To determine which of these solutions is realized in practice, some additional analysis of their stability is needed.

FUNDING

REFERENCES

1. Yu. A. Altukhov, A. S. Gusev, and G. V. Pyshnograi, *Introduction to the Mesoscopic Theory of Flowing Polymer Systems* (Altai State Pedagogical Academy Press, Barnaul, 2012) [in Russian].
2. V. N. Pokrovskii, *The Mesoscopic Theory of Polymer Dynamics* (Springer, Berlin, 2010).
3. G. V. Vinogradov, V. N. Pokrovskii, and Yu. G. Yanovsky, "Theory of Viscoelastic Behavior of Concentrated Polymer Solutions and Melts in One-Molecular Approximation and Its Experimental Verification," Rheol. Acta **7**, 258−274 (1972).

4. L. G. Loitsyanskii, *Mechanics of Liquids and Gases* (Stewartson Pergamon Press, Oxford, 1966; Nauka, Moscow, 1978).
5. S. A. Zinovich, I. E. Golovicheva, and G. V. Pyshnograi, "Influence of the Molecular Weight on the Shear Viscosity and Longitudinal Viscosity of Linear Polymers," Prikl. Mat. i Tekhn. Fiz. **41** (2), 154−160 (2000).
6. B. Y. Ahn, S. B. Walker, S. C. Slimmer, et al., "Planar and Three-Dimensional Printing of Conductive Inks," J. Vis. Exp. **58**, 3189 (2011).
7. S. D. Hoath, W.-K. Hsiao, G. D. Martin, et al., "Oscillations of Aqueous PEDOT:PSS Fluid Droplets and the Properties of Complex Fluids in Drop-on-Demand Inkjet Printing," J. Non-Newtonian Fluid Mechanics. **223**, 28−36 (2015).
8. H.-H. Lee, K.-S. Chou, and K.-C. Huang, "Inkjet Printing of Nanosized Silver Colloids," Nanotechnology **16**, 2436−2441 (2005).
9. P. K. Kahol, J. C. Ho, Y. Y. Chen, et al., "On Metallic Characteristics in Some Conducting Polymers," Synthetic Metals **151** (2), 65−72 (2005).
10. T.-H. Le, Y. Kim, and H. Yoon, "Electrical and Electrochemical Properties of Conducting Polymers," Polymers **9** (4), No. 150 (2017).
11. K. Muro, M. Watanabe, T. Tamai, et al., "PEDOT/PSS Nano-Particles: Synthesis and Properties," RSC Adv. **6** (90), 87147−87152 (2016).
12. D. G. Yoon, M. G. Kang, J. B. Kim, et al., "Nozzle Printed-PEDOT:PSS for Organic Light Emitting Diodes with Various Dilution Rates of Ethanol," Appl. Sci. **8** (2), 203 (2018).
13. A. N. Papathanassiou, I. Sakellis, J. Grammatikakis, et al., "Exploring Electrical Conductivity Within Mesoscopic Phases of Semiconducting PEDOT:PSS Films by Broadband Dielectric Spectroscopy," Appl. Phys. Lett. **103**, 123304 (2013).
14. J. Liu, X. Wang, D. Li, et al., "Thermal Conductivity and Elastic Constants of PEDOT:PSS with High Electrical Conductivity," Macromolecules **48** (3), 585−591 (2015).
15. N. Z. Khan, "Modeling and Simulation of Organic Mem Relay for Estimating the Coefficient of Thermal Expansion of PEDOT: PSS," TechConnect Briefs. **4**, 120−123 (2017).
16. B. V. Semisalov, "A Nonlocal Algorithm for Finding a Solution to the Poisson Equation and Its Applications," Zh. Vychisl. Mat. i Mat. Fiz. **54** (7), 1110−1135 (2014).
17. B. V. Semisalov, "Computing Code for Finding Solutions to Boundary Value Problems for Partial Differential Equations with High Accuracy and Low Computational Costs 'Nonlocal Method Without Saturation'," State Registration Certificate No. 2015615527 Issued on May 20, 2015.
18. B. V. Semisalov, "Fast Nonlocal Algorithm for Solving Neumann−Dirichlet Boundary Value Problems with an Error Control," Vychisl. Metody. Programmirovanie **17** (4), 500−522 (2016).
19. B. V. Semisalov, "Development and Analysis of the Fast Pseudo Spectral Method for Solving Nonlinear Dirichlet Problems," Bull. South Ural State University. Ser. Math. Modelling, Program. Comp. Software. **11** (2), 123−138 (2018).
20. L. I. Sedov, *Mechanics of Continuous Media* (Nauka, Moscow, 1970; World Scientific, 1997).
21. A. B. Vatazhin, G. A. Lyubimov, and S. A. Regirer, *Magnetic Hydrodynamic Flows in Channels* (Nauka, Moscow, 1970) [in Russian].
22. Shih-I. Pai, *Introduction to the Theory of Compressible Flow* (Literary Licensing, Whitefish, 2013).
23. A. M. Blokhin and A. S. Rudometova, "Stationary Flows of a Weakly Conducting Incompressible Polymeric Liquid Between Coaxial Cylinders," Sibir. Zh. Industr. Mat. **20** (4), 13−21 (2017) [J. Appl. Indust. Math. **17** (4), 486−493 (2017)].
24. A. M. Blokhin and A. S. Rudometova, "Stationary Solutions of the Equations for Nonisothermal Electroconvection of a Weakly Conducting Incompressible Polymeric Liquid," Sibir. Zh. Industr. Mat. **18** (1), 3−13 (2015) [J. Appl. Indust. Math. **9** (2), 147−156 (2015)].
25. A. I. Akhiezer and I. A. Akhiezer, *Electromagnetism and Electromagnetic Waves* (Vysshaya Shkola, Moscow, 1985) [in Russian].
26. K. Nordling and J. Österman, *Physics Handbook for Science and Engineering* (Studentlitteratur, Lund, 1999; BXB-Peterburg, St. Petersburg, 2011).
27. Y. Shibata, "On the r-Boundness for the Two Phase Problem with Phase Transitions: Compressiable−Incompressiable," Model Problem. Funkcialaj Ekvacioj. **59**, 243−287 (2016).
28. A. M. Blokhin, B. V. Semisalov, and A. S. Shevchenko, "Stationary Solutions of the Equations Describing Nonisothermal Convection of an Incompressible Polymeric Viscous-Elastic Liquid," Mat. Model. **28** (10), 3−22 (2016).
29. A. M. Blokhin, E. A. Kruglova, and B. V. Semisalov, "Steady-State Flow of an Incompressible Viscoelastic Polymeric Fluid Between Two Coaxial Cylinders," Comp. Math. Math. Physics (2017) **57** (7), 1181−1193.
30. S. G. Kalashnikov, *Electricity* (Nauka, Moscow, 1964) [in Russian].
31. R. Kubo, *Thermodynamics: An Advanced Course with Problems and Solutions* (North Holland, Amsterdam 1968; Mir, Moscow, 1970).